RADIOAUTOGRAPHIC ANALYSIS OF THE SECRETORY PROCESS IN THE PAROTID ACINAR CELL OF THE RABBIT

J. DAVID CASTLE, JAMES D. JAMIESON, and GEORGE E. PALADE

From The Rockefeller University, New York 10021

ABSTRACT

Intracellular transport of secretory proteins has been studied in the parotid to examine this process in an exocrine gland other than the pancreas and to explore a possible source of less degraded membranes than obtainable from the latter gland. Rabbit parotids were chosen on the basis of size (2–2.5 g per animal), ease of surgical removal, and amylase concentration. Sites of synthesis, rates of intracellular transport, and sites of packaging and storage of newly synthesized secretory proteins were determined radioautographically by using an in vitro system of dissected lobules capable of linear amino acid incorporation for 10 hr with satisfactory preservation of cellular fine structure. Adequate fixation of the tissue with minimal binding of unincorporated labeled amino acids was obtained by using 10% formaldehyde–0.175 M phosphate buffer (pH 7.2) as primary fixative. Pulse labeling with leucine-^{3}H, followed by a chase incubation, showed that the label is initially located (chase: 1–6 min) over the rough endoplasmic reticulum (RER) and subsequently moves as a wave through the Golgi complex (chase: 16–36 min), condensing vacuoles (chase: 36–56 min), immature granules (chase: 56–116 min), and finally mature storage granules (chase: 116–356 min). Distinguishing features of the parotid transport apparatus are: low frequency of RER-Golgi transitional elements, close association of condensing vacuoles with the exit side of Golgi stacks, and recognizable immature secretory granules. Intracelular processing of secretory proteins is similar to that already found in the pancreas, except that the rate is slower and the storage is more prolonged.

INTRODUCTION

The parotid, the only entirely serous major salivary gland in most mammals, possesses a cellular organization very similar to that of the exocrine pancreas. In the latter the kinetics of intracellular transport of newly synthesized secretory protein has been clearly defined by radioautography and cell fractionation (1–6). The entire process of synthesis, concentrative packaging, storage, and release takes 1–2 hr. However, more detailed studies of the membranes of the pancreatic subcellular components involved in transport are handicapped by apparently uncontrollable endogenous lipolytic degradation (7) and potential proteolytic degradation resulting from leakage and activation of protease zymogens.

We have undertaken a radioautographic study of the rabbit parotid gland in vitro principally (*a*) to test on another cell type the kinetics of intracellular transport worked out for the pancreatic acinar cell, and (*b*) to explore a system in which membrane lipolytic and proteolytic degradation is not expected.

Morphological, biochemical, and cytochemical studies on rat parotid (8–13) suggested that the

same subcellular compartments and same over-all schedule are involved in the processing of secretory protein in the two kinds of acinar cells; however, precise information concerning the route and timetable followed by secretory proteins in the parotid was, until now, missing.

MATERIALS AND METHODS

Animals

The rabbit was selected as experimental animal on the basis of gland size and amylase concentration as seen in Table I. Furthermore, the well-defined connective tissue capsule of the rabbit parotid facilitates surgical removal. 4–5-lb. male New Zealand white rabbits, fed *ad libitum*, were sacrificed with an overdose of sodium pentobarbital injected into the ear vein. Both parotid glands were removed and placed immediately in chilled incubation medium. External connective tissue, lymph nodes, and fat were dissected away in incubation medium at 4°C.

Instead of using thin tissue slices (5, 6) we used dissected lobules for in vitro incubation. The excised glands were distended by injecting incubation medium into their stroma, and tiny individual lobules (1 × 2 × 3 mm) rendered visible by this inflation were dissected, taking care to cut through duct and connective tissue, thus minimizing damage to acini.

Incubation Procedures

Incubation conditions differed with the design of the experiment as follows:

CONTINUOUS INCORPORATION OF LABELED LEUCINE: Dissected lobules were placed in 25-ml Erlenmeyer flasks (seven to nine lobules per flask) containing 5 ml of Nutrient Mixture F 12 (referred to subsequently as F 12), a chemically defined synthetic medium (14), supplemented with L-leucine-4,5-^{3}H at 5 μCi/ml. Flasks containing lobules and medium were gassed with 95% O_2 + 5% CO_2 (pH 7.2) and kept on ice for 10 min. At the onset of incubation, the flasks were transferred to a 37°C water bath and agitated at 70 cycles/min. The O_2 + CO_2 atmosphere was maintained either by continuous gas flow or by intermittent gassing at 20- 30-min intervals. For long-term incubation 100 units/ml penicillin and 0.05 mg/ml streptomycin were added to the medium to prevent bacterial growth. At specified time points lobules were removed, washed with isotonic NaCl, and homogenized in 2.0 ml H_2O to provide samples for chemical and radioactivity assays.

MORPHOLOGY: To study the fine structure of the in vitro incubated parotid, two to three lobules were incubated as described above, except that label was omitted. At selected time points the tissue was placed directly into hypertonic aldehyde fixative. The lobules were diced in the fixative and processed for electron microscopy.

RADIOAUTOGRAPHY: To introduce a short well-defined pulse of radioactivity into secretory protein with leucine-^{3}H, it was necessary to deplete the tissue's endogenous pool of unlabeled leucine before and during pulse incubation. Since commercial F 12 contains 0.1 mM L-leucine, we used instead Krebs-Ringer-bicarbonate (KRB) medium supplemented with all amino acids (except leucine) at concentrations found in Eagle's minimal essential medium; during the pulse, L-leucine-4,5-^{3}H (54 Ci/mmole) was present at a concentration of 300 μCi/ml (5.4 μM), previously determined to be sufficient for EM radioautography. Dissected lobules that had been incubated 10 min at 0°C in leucine-free medium before pulse were transferred to 4 ml of gassed pulse medium in a 10 ml Erlenmeyer flask. After a 5–10 min equilibration at 0°C the pulse flask was warmed to 37°C for 4 min. Lobules were then immediately washed in a large volume (~200

TABLE I
Size and Amylase Content of Parotid Glands of Various Mammals

Animal	Body weight	Wet weight (Pair of parotids)	Specific activity of amylase in glands	
			units*/mg protein	units*/mg DNA
Rat	160	0.8	1.85×10^2	2.41×10^4
Guinea pig	270	0.3	0.47×10^2	0.84×10^3
Hamster	100	0.2	0.95×10^2	0.43×10^4
Rabbit	~2300	2–2.5	0.65×10^2	1.68×10^4

Parotids were quickly removed from sacrificed animals and placed in 0.9% NaCl. After excess connective tissue, lymph nodes, and fat were dissected away, the glands were weighed and then diced and homogenized extensively in distilled water (2.0 ml/0.3 g wet weight of gland). Samples were taken for assays of amylase activity, total protein, and DNA.

* 1 unit of amylase activity = 1 mg maltose produced/3 min at 30°C.

ml) of F 12 supplemented with leucine-^{1}H to a concentration of 4 mM, and subjected to chase incubation (37°C and 70 cycles/min) in 20 ml of this same medium in 125-ml Erlenmeyer flasks. At specified time points tissue was removed and immersed in hypertonic, phosphate-buffered formaldehyde. The ratio of leucine concentration in the chase medium to leucine concentration in the pulse medium was ~750, while the volume dilution from pulse to chase was fivefold.

STIMULATED DISCHARGE OF SECRETORY PRODUCT: To estimate the partitioning of incorporated leucine-^{3}H between exportable and nonexportable proteins, parotid lobules were pulse labeled and then chased for the time required (3 hr) to bring labeled secretory proteins into secretion granules. At that time isoproterenol (a powerful sympathomimetic stimulant of parotid secretion [10, 15–17]) was added to a final concentration of 1 μM, and the incubation was continued for 4 hr. Percentage release of protein radioactivity and amylase into the medium was determined, using discharge assays previously reported (18). Separate dose-response experiments had shown that the optimal isoproterenol concentration for our system was 1 μM.

Tissue Processing for Microscopy

Tissue, excluding lobules for radioautography, was initially fixed for 4–20 hr at room temperature in either 4% glutaraldehyde or 2% formaldehyde + 2% glutaraldehyde buffered to pH 7.2 with hypertonic potassium phosphate (0.15–0.2 M) or with sodium cacodylate (0.15–0.2 M) (19). We found in preliminary work that hypertonic conditions are necessary to reduce swelling, explosion, and extraction of secretory granules. Tissue was then postfixed 3–4 hr at 0°C in 1% osmium tetroxide buffered to pH 7.2 as described above, washed twice in 0.17 M NaCl, stained in-block for 60 min at 0°C with 0.5% magnesium uranyl acetate in 0.17 M NaCl, dehydrated in ethanol, and embedded in Epon (20). Sections, 0.5 μ thick, were stained in 1% methylene blue–1% sodium borate (21) and used for surveying the material before cutting thin (silver) sections for electron microscopy. Thin sections were stained in alcoholic uranyl acetate and alkaline lead citrate (22) and observed in a Siemens Elmiskop I.

For radioautography, lobules were initially fixed in 10% formaldehyde in 0.175 M potassium phosphate (pH 7.2), using five to six changes to promote extraction of unincorporated label. Bifunctional aldehydes were omitted to minimize the binding of unincorporated leucine-^{3}H (23, 24). Tissue was postfixed, dehydrated, and embedded as described above, except that in-block staining with magnesium uranyl acetate was omitted.

Light microscope (LM) radioautography was initially performed as previously described (6) on 0.5 μ thick Epon sections affixed to glass slides to provide an estimate for length of exposure necessary to produce sufficient silver grains for electron microscope (EM) radioautography. In general, the number of days of exposure required to yield an adequate grain count for LM radioautography approximates the number of weeks necessary for exposure for EM radioautography.

After satisfactory assessment of LM radioautographs, pale gold sections were cut, collected on 200-mesh copper grids (Formvar- and carbon coated), and covered with Ilford L4 photographic emulsion, using the method of Caro and van Tubergen (25). Exposure was performed in light-tight boxes at 4°C. After photographic processing and hydrolysis of emulsion gelatin (by 20 min immersion in 0.1 N NaOH), the sections were doubly stained (22) and micrographed at low magnification in a Siemens Elmiskop I. Grain counts on the resultant micrographs were used to quantitate the results.

Radioactivity Assay and Chemical Assays

RADIOACTIVITY: Samples of tissue homogenate and incubation media were precipitated with trichloracetic acid (TCA) at 10% final concentration, 0.5 N perchloric acid (PCA), or 0.5 N PCA-0.5% phosphotungstic acid (PTA) and kept for at least 2 hr at 4°C. The precipitates were then pelleted by centrifugation and washed twice by resuspension and repelleting in the appropriate cold acid. Drained pellets were dissolved in 0.3 ml 88% formic acid (where TCA or PCA served as precipitant) or 0.5 ml *N*-chlorosuccinimide (where PCA-PTA served as precipitant). Acid-soluble fractions and the dissolved precipitates were counted in a *p*-dioxane base liquid scintillation fluid (26), using a Nuclear-Chicago Mark I liquid scintillation spectrometer. Counting rates were corrected for quenching (with an external standard) and for background.

CHEMICAL: Amylase was assayed according to the method of Bernfeld (27) on samples of tissue homogenates diluted with 0.2% Triton X 100 containing 0.02 M sodium phosphate (pH 6.9) and 0.02 M NaCl.

Total protein was determined according to Lowry et al. (28) on samples of TCA precipitates of homogenates dissolved in 1 N NaOH. Crystalline bovine plasma albumin was used as standard.

DNA content was determined by Burton's method (29) on hot 0.5 N PCA extracts of washed PCA precipitates of samples of tissue homogenate. Calf thymus DNA was used as standard.

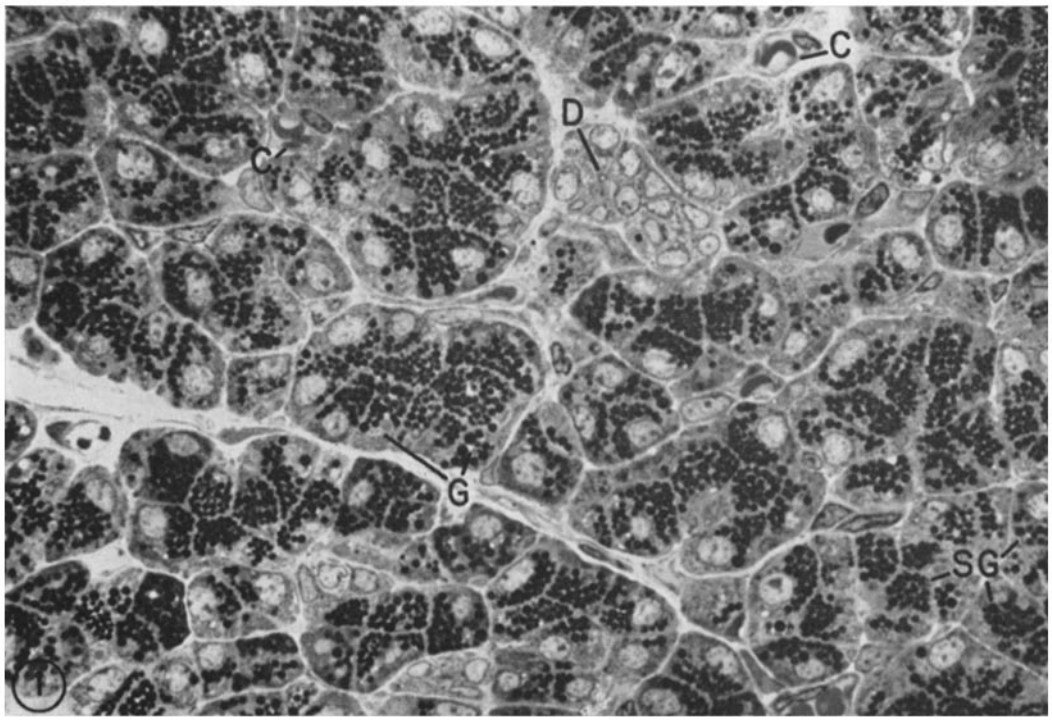

FIGURE 1 Light micrograph of parotid tissue showing the compact organization of the lobules. Acini are almost exclusively composed of acinar cells containing basally located nuclei and ergastoplasm and extensive apical accumulations of secretory granules (*SG*). Faintly stained areas representing Golgi complexes (*G*) are observed both subapically and immersed in the granule population. Profiles of acinar lumina are not evident at the cellular apices due to the distended state of the cells. Occasional ducts (*D*) and capillaries (*C*) penetrate the interacinar and interlobular spaces. Epon section (0.5 μ) of fresh tissue fixed initially with 4% glutaraldehyde in 0.1 M K phosphate (pH 7.2) and postfixed in 1% OsO_4 in the same buffer; stained with 1% methylene blue in 1% Na borate. × 730.

Materials

L-leucine-4,5-^{3}H (specific activity 50–58 Ci/mmole) and isoproterenol hydrochloride were purchased from Schwarz Bio Research Inc., Orangeburg, N. Y. Nutrient Mixture F 12 was obtained in liquid form from Grand Island Biological Co., Grand Island, N.Y. and in powder form from Schwarz Bio Research Inc. Ilford L4 liquid photographic emulsion was obtained from Ilford Ltd., Ilford, Essex, England.

RESULTS

As can be seen in Fig. 1, the rabbit parotid is predominantly composed of closely packed acini. Ducts are few in number and blood vessels and cellular elements of the connective tissue occur at low incidence in the narrow interacinar and interlobular spaces. With the exception of infrequently encountered myoepithelial cells, a single cell type, the acinar cell, is the main constituent of the tissue and accounts for 91% of the lobule volume. The remainder consists of ducts (3%), blood vessels (4%), and connective tissue cells (2%).[1] Evidently this tissue is considerably less heterogeneous than the liver; it is slightly more homogeneous than the pancreas, having the further advantage over the latter of containing a single secretory cell type.

Morphology of Acinar Cells

The acinar cells have the shape of irregular, truncated pyramids whose apices are directed

[1] Volume approximations are weight percentages determined from 12 light micrographs (total tissue area 2 × 10^4 μ^2) by cutting out and weighing the profiles of tissue elements.

toward the acinar lumina. At the subcellular level they have the characteristic organization of cells producing and accumulating protein for secretion. As illustrated by Fig. 2, they have a well-developed rough endoplasmic reticulum (RER) arranged in arrays of parallel cisternae and a large population of polysomes and ribosomes which is predominantly membrane bound. Their Golgi complex is extensive and consists of the usual elements (stacks of cisternae, small peripheral vesicles, and large condensing vacuoles), but its location and orientation is more variable than in other exocrine cells (3, 5, 23, 30, 31). The secretory granules, which occupy half or more of the cell volume even in animals fed *ad libitum*, are large and variable in dimensions (1.1–1.5 μ diameter) and irregular in shape (see Fig. 2). They are closely packed and frequently deformed by contact with one another. According to their content they can be classified in two groups. The first has a homogeneous content, occupies the apical region proper, and represents mature granules. The second has a heterogeneous content (see legends, Figs. 10, 11), is located subapically usually in the vicinity of the Golgi complex and, as will be shown, represents immature granules. The acinar lumina appear to be either branched or highly contorted since in sections a single cell often appears associated with more than one luminal profile (Figs. 6, 7). The first alternative is supported by the light microscopy literature in which branched intercellular secretory capillaries have been described in the mammalian parotid (32). The cell surface is provided with microvilli on the apical aspect, with typical junctional complexes located laterally in the immediate vicinity of the lumen, and with an elaborate system of narrow interdigitating outfoldings extending over the entire lateral surface basal to the complexes. Only the basal aspect is partially free of such protrusions. The nucleus is located in the basal half of the cell, usually surrounded by arrays of rough ER cisternae.

The following features appear to distinguish the acinar cell of the rabbit parotid from that of the guinea pig pancreas: (*a*) intracisternal granules consistently observed at low incidence in tissue fixed *in situ* or incubated in vitro before fixation; (*b*) variable location and orientation of the Golgi complex;[2] (*c*) stacks of flattened Golgi cisternae extending over large areas with peripheral vesicles and especially transitional elements less numerous than in pancreatic exocrine cells; (*d*) frequent coated vesicles located in the vicinity of the exit side of the Golgi complex; (*e*) the presence of immature granules identifiable by their heterogeneously packed content; (*f*) multiple luminal profiles per acinar cell section.

Morphology of In Vitro Incubated Parotid Lobules

Light- and electron microscope observations of the lobules incubated for up to 12 hr show that the general organization of lobules, acini, and acinar cells is quite well preserved. Through 4 hr the appearance of the acinar cells remains essentially unaltered. From 4 to 12 hr the following progressive changes take place: (*a*) swelling of individual RER cisternae and disorganization of cisternal arrays; (*b*) swelling and vesiculation of Golgi cisternae; (*c*) nuclear pycnosis; and (*d*) formation of large cytoplasmic vacuoles. A few cells are obviously disrupted and extracted. By 12 hr of incubation acinar cells generally show nuclear pycnosis and vesiculation of Golgi elements, but only 10–20% exhibit the other changes mentioned above. The secretory granules are well preserved in nearly all intact cells.

Incorporation of Leucine-^3H into Total Lobule Proteins during In Vitro Incubation

When parotid lobules were incubated at 37°C in gassed F 12 supplemented with 5 μCi/ml L-leucine-^{3}H, label was incorporated into protein at a constant rate (very similar to that observed with pancreatic slices [18]) for at least 8 hr (Fig. 3). Thus the protein-synthesizing apparatus remains generally and consistently active in lobules subjected to prolonged incubation. On morphological and biochemical grounds this system is directly comparable to that used for in vitro in-

[2] From extensive EM observations we have the impression that the large Golgi complex of the rabbit parotid exocrine cell has a variable relationship with other cell organelles. In sections it is frequently located lateral, rather than apical, to the nucleus or often appears immersed in the mass of accumulated granules. Its area of contiguity with the RER is small, and its exit side is not consistently directed toward the mass of stored granules. These variations may reflect the preferred orientation of the complex (or complexes—since the cell may have more than one Golgi complex) toward the multiple secretory lumina with which the cell is associated (Fig. 7).

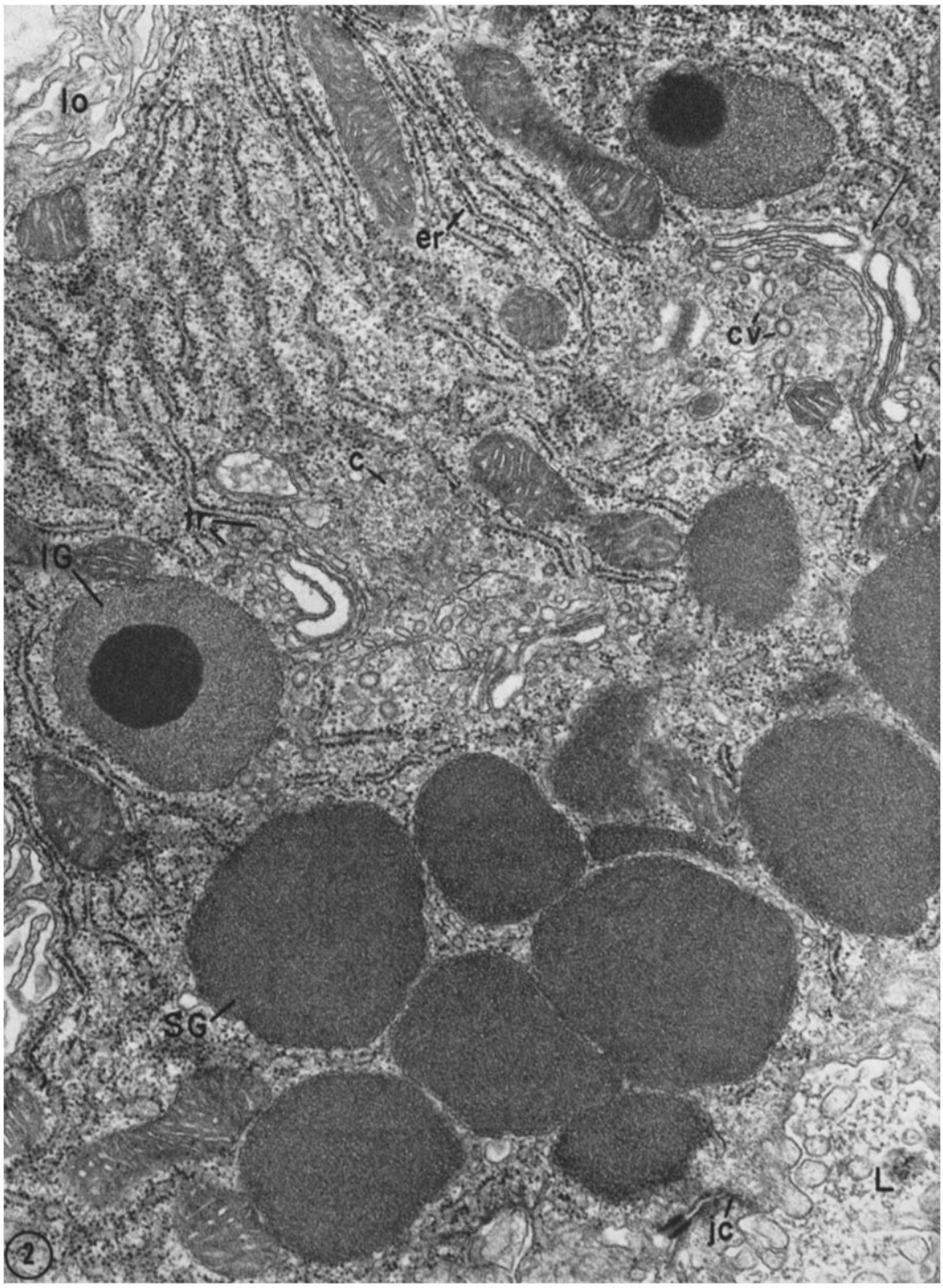

FIGURE 2 Electron micrograph of the apical portion of a rabbit parotid acinar cell. Note the parallel arrays of RER cisternae (*er*); the RER-Golgi transitional elements (*tr*); the components of the Golgi complex–peripheral vesicles (*v*), parallel flattened cisternae showing interconnections (arrow), and condensing vacuole (*c*); the coated vesicles (*cv*) located mostly near the exit side of the Golgi complex; the immature granules (*IG*) containing heterogeneously packed content; the mature secretory granules (*SG*), irregularly shaped and closely packed; the acinar lumen (*L*) and junctional complexes (*jc*); and the lateral plasma membrane outfoldings (*lo*). Initial fixation in 4% glutaraldehyde–0.15 M Na cacodylate (pH 7.2). × 25,000.

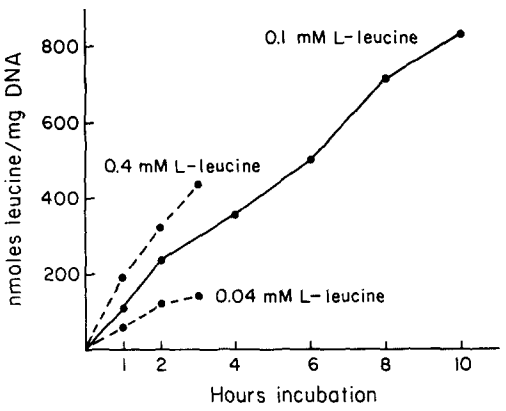

FIGURE 3 Incorporation of L-leucine-^{3}H into total lobule proteins. Lobules were incubated in F 12 (containing 0.1 mM L-leucine-^{1}H) supplemented with 5 μCi/ml L-leucine-^{3}H (58 Ci/mmole). At the indicated times the incubation was terminated and lobules and incubation medium were separated for assay. Samples of the medium were precipitated with TCA (10% final concentration) after adding 1 mg/ml carrier bovine plasma albumin. The lobules were homogenized in water, and homogenate samples were precipitated with 10% TCA for assay of radioactivity and 0.5 N PCA for DNA determinations. Total leucine incorporated into protein was calculated from the disintegrations per minute found in proteins in the lobules plus the medium and from the specific radioactivity of leucine-^{3}H in the medium. The solid line depicts results obtained for parotid lobules when the concentration of leucine in the incubation medium was 0.1 mM. The broken lines represent data obtained with guinea pig pancreatic slices incubated in amino acid supplemented KRB containing 5 μCi/ml leucine-^{3}H (58 Ci/mmole) and either 0.04 or 0.4 mM leucine-^{1}H (see Fig. 8 in reference 18).

corporation studies on guinea pig pancreatic slices (5, 6, 18).

Pulse-Chase Characteristics of Parotid Lobules

As previously discussed (5), a study of the intracellular transport of secretory proteins requires: (*a*) pulse labeling obtained by brief exposure to labeled precursors (shorter than the shortest time intervals involved in transport from one intracellular compartment to another) followed by the washout of the unincorporated label by transfer of the tissue to a chase medium; (*b*) a large difference between the rates of synthesis of exportable and nonexportable proteins.

To determine if pulse labeling could be successfully achieved in our in vitro system, dissected lobules were subjected in succession to prepulse incubation at 0°C for 10 min in a leucine-free medium, equilibration at 0°C for 10 min in tracer-containing medium, pulsing by warming to 37°C for 4 min, extensive washing with leucine-^{1}H–supplemented chase medium, and finally chase incubation for times up to 80 min. The results (Fig. 4) show that chase incubation is successful in promoting both rapid washout of cold PCA-PTA–soluble radioactivity and cessation of incorporation of radioactive leucine into proteins.[3] The chase is fully satisfactory, and the rate of washout is comparable to that for pancreatic slices. In the first 5 min 78% of the initial amount of unincorporated label is washed out from parotid lobules and 73% from pancreatic slices. The final amount of labeled precursor remaining in parotid lobules after cessation of chase incubation is two orders of magnitude below the initial postpulse value.

To assess whether there is a large difference in the relative amounts of leucine-^{3}H incorporated into secretory and nonsecretory proteins in parotid acinar cells, we subjected lobules in succession to pulse labeling, chase incubation of sufficient duration to label secretory granules, and further incubation in the presence or absence of 1 μM isoproterenol to determine the percentages of incorporated radioactivity and amylase discharged (18). Fig. 5 shows that through the first 2 hr of incubation in the presence of isoproterenol 61% of the protein radioactivity and 90% of total amylase are released into the incubation medium. During subsequent incubation from 2 to 4 hr an additional 5% of both incorporated radioactivity and amylase appears in the medium at a rate comparable to that of secretion from unstimulated lobules. Thus we estimate that during the pulse two-thirds of the labeled protein precursor is incorporated into secretory protein eventually exported from acinar cells. The remaining one-third of the radioactivity represents both nonsecretory protein retained for intracellular use and additional secretory protein not yet cleared from the intracellular transport system.[4]

[3] PTA was found to be a necessary additive to precipitate large labeled molecules which progressively accumulate for the duration of chase incubation and which were not precipitable by PCA or TCA alone.

[4] The morphologic aspects of isoproterenol-induced secretion will be the subject of a later communication.

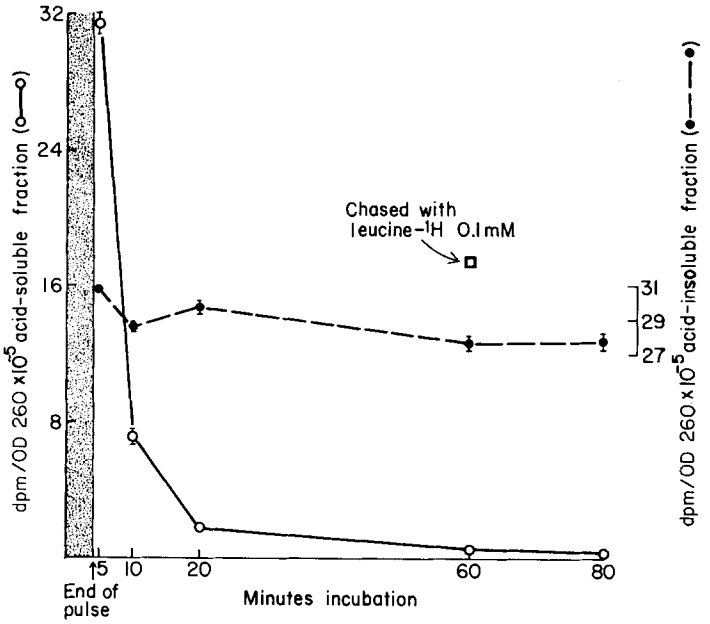

FIGURE 4 Kinetics of pulse labeling of parotid lobule proteins. The prepulse incubation medium was KRB (25 ml) supplemented with all amino acids except leucine. The pulse medium contained 50 μCi/ml L-leucine-4,5-^{3}H (1 μM) and leucine-^{1}H (4 μM). The wash and chase medium was F 12 with added leucine-^{1}H to a final concentration of 4 mM. The pulse:chase ratio of leucine concentration is comparable to that used in our radioautographic experiments. The chase of unincorporated leucine-^{3}H (cold PCA-PTA–soluble radioactivity) is indicated by the open circles and solid line. Incorporated leucine-^{3}H (cold PCA-PTA–insoluble radioactivity) is shown by the closed circles and broken line. The results (averaged from duplicate samples) are expressed relative to OD 260 of hot PCA extracts of samples of tissue homogenates initially precipitated and washed with cold PCA. A single sample (shown by the open square) was chased up to 60 min with F 12 containing 0.1 mM leucine-^{1}H and demonstrates the reduced chaseability of acid-insoluble radioactivity at lower leucine concentrations. Disintegrations per minute, *dpm*.

Binding of Soluble (Unincorporated) L-leucine-4,5-^{3}H during Fixation for Radioautography

To obtain satisfactory structural preservation we were obliged to use aldehydes as primary fixatives. OsO_4 alone, even in hypertonic solutions, did not prevent the swelling and disruption of secretory granules. Since significant binding of unincorporated leucine-^{3}H and glucosamine-^{3}H during fixation in the presence of glutaraldehyde has been reported in the radioautographic studies of Ashley and Peters on rat liver (24) and Wuhr et al. (23) on rat thyroid, it was necessary to assess the extent of binding of soluble label during tissue fixation. Such binding represents a potential source of error in radioautography for specimens fixed either at the end of the pulse or after a short chase incubation.

Parotid lobules were pulsed for 4 min under three different conditions: (*1*) normal pulse at 37°C, (*2*) pulse at 37°C in the presence of 5×10^{-4} M cycloheximide (CHI) known to inhibit protein synthesis by 95–98% in guinea pig pancreatic slices (33), and (*3*) pulse at 0°C. After the pulse, lobules were fixed in several changes of either 2% glutaraldehyde + 2% formaldehyde or 10% formaldehyde (24). The fixed tissue was weighed and dissolved in hot 1 N NaOH; the digest was assayed for radioactivity. Label bound in the absence of protein synthesis (pulse conditions *2* and *3*) is assumed to approximate the level of chemical (fixative) binding expected in radioautographic experiments. The results are expressed in Table II as percentage of the specific radioactivity of specimens pulsed under normal conditions and fixed postpulse in 10% formaldehyde. The table shows that the presence of glutaralde-

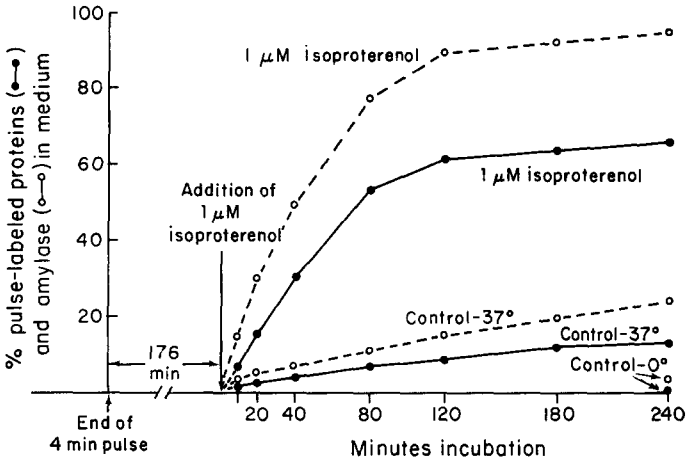

FIGURE 5 Discharge of leucine-^{3}H-labeled secretory protein from parotid lobules. Lobules were labeled for 4 min in pulse medium containing 300 μCi/ml L-leucine-4,5-^{3}H (5.4 μM) washed and chase incubated in F 12 supplemented with leucine-^{1}H (4 mM final concentration) for 176 min to allow the labeled secretory proteins to reach the secretion granule stage, and then divided into three groups and incubated further in leucine-supplemented F 12 in the presence (at 37°C) or absence (at 0°C and 37°C) of 1 μM isoproterenol to stimulate discharge of granule content. At the specified times, 2-ml samples of incubation media were removed and immediately replaced by the same volume of fresh medium. Isoproterenol was included in the replacement medium to compensate for secretagogue depleted by medium removal and by oxidation. The medium samples collected during incubation as well as the tissue at the end of incubation were assayed for protein radioactivity and amylase. Percentage release of labeled protein and amylase was calculated from the data obtained. Note the very low level of release of amylase from lobules during prolonged 0°C exposure, which demonstrates that the enzyme leakage observed by Schramm et al. (43) is not a problem in our system. For the sake of graphical clarity we have plotted only the final points for the 0°C control. Release at 0°C of labeled protein and amylase increases monotonically to the final values of 0.5% and 4%, respectively.

hyde in the fixative increases the specific activity of bound label by 57% for tissue pulsed under normal conditions and increases binding eightfold in tissue pulsed at 0°C in the absence of protein synthesis. Chemical binding of the leucine-^{3}H by the fixative used throughout our radioautographic experiments (i.e., 10% formaldehyde–0.175 M potassium phosphate, pH 7.2) accounts for, at maximum, 10% of the tissue-associated radioactivity. This figure can be expected to decrease with increasing times of chase incubation. Thus we can assume that in our experiments radioautographic grains primarily localize label incorporated into protein and that errors induced by chemical binding are negligible.

Radioautographic Studies

Since we found that true pulse labeling and effective chase could be achieved by the in vitro incubation of rabbit parotid lobules and that binding of unincorporated and unchased leucine-^{3}H was minimal, we performed radioautographic studies to determine rates of intracellular transport and of compartment drainage. Our kinetic analysis can be directly compared to that achieved with guinea pig pancreatic slices (6).

Parotid lobules were pulse labeled for 4 min with L-leucine-4,5-^{3}H (300 μCi/ml; 5.4 μM) and incubated postpulse for times ranging from 1 to 356 min in chase medium containing 4 mM L-leucine-^{1}H. During tissue fixation and subsequent preparation for electron microscopy, label extraction was monitored in parallel samples by following the radioactivity which appeared in fixing and dehydrating fluids and comparing it with that remaining in completely processed, Epon-infiltrated tissue subsequently dissolved in hot 1 N NaOH. The dissolved tissue accounted for 90% of the radioactivity, the aldehyde fixatives for 6–7%, and the subsequent osmium tetroxide fixative and dehydrating and Epon equilibration

TABLE II

Binding of Unincorporated Leucine-^3H to Tissue by Aldehyde Fixatives

Experiment	Sample	Aldehyde fixative	% of specific activity
I	Normal pulse	10% formaldehyde	100*
	Pulse in CHI	10% formaldehyde	10
	Pulse at 0°C	10% formaldehyde	2
II	Normal pulse	10% formaldehyde	100*
	Pulse at 0°C	10% formaldehyde	6
	Normal pulse	2% formaldehyde + 2% glutaraldehyde	157
	Pulse at 0°C	2% formaldehyde + 2% glutaraldehyde	46

* 100% is arbitrarily chosen as the specific activity of label found in lobules subjected to normal pulse incubation followed by fixation in 10% formaldehyde. It corresponds to specific activities of 142,000 dpm/mg wet weight in experiment I and 75,300 dpm/mg wet weight in experiment II.

For all conditions the pulse medium consisted of KRB supplemented with amino acids, L-leucine-^3H being present at a concentration of 300 μCi/ml (5.4 μM); for condition 2, experiment I only, cycloheximide (CHI) was added to a final concentration of 5×10^{-4} M. The prepulse incubation medium was leucine free. Aldehyde fixation was performed for 22 hr in either 10% formaldehyde buffered by 0.2 M (experiment I) or 0.175 M (experiment II) phosphate (pH 7.2) or in 2% formaldehyde–2% glutaraldehyde 0.175 M K phosphate (pH 7.2).

fluids for 3% (total). Thus label retention during tissue processing is very nearly complete.

LIGHT MICROSCOPE RADIOAUTOGRAPHY: Thick sections, 0.5 μ, were cut from tissue at all time points and prepared for radioautography. These specimens indicate in a general way the movement of incorporated leucine-^3H from basal cytoplasm (chase: 1–6 min) to the centrosphere region (chase: 11–56 min) to secretory granules located primarily in the basal part of the granule accumulation (chase: 56 min and longer). Adequate grain density at the light microscope level was obtained with 6 days of exposure for samples chased for 1–116 min and with 9 days of exposure for samples chased for 176–356 min. Thus approximately 6 and 9 wk of exposure are required for radioautography at the EM level.

LM radioautography showed that lobules were not uniformly labeled during the leucine-^3H pulse: a gradient of label from their periphery to their center was observed with centermost acini showing lower grain density. Nevertheless, the rate of intracellular processing of label was uniform throughout the thickness of the lobule despite the uneven penetration of leucine-^3H. Thus it can be concluded that the intracellular transport of incorporated label is carried out in synchrony in the entire cell population.

ELECTRON MICROSCOPE RADIOAUTOGRAPHY: EM radioautography was performed on thin sections cut from the same material used for LM radioautography.

After 1 min chase (Fig. 6) the label was localized over the rough endoplasmic reticulum (RER) with relatively few grains appearing over the Golgi complex and secretory granules.

By 11 min chase (Fig. 7), a large fraction of the label had converged to the smooth membranes of the Golgi complex, although the majority of the grains was still associated with the RER.

After 26 min chase incubation (Fig. 8) labeled protein was primarily associated with the Golgi complex. Radioautographic grains marked all the elements of the complex including its stacked cisternae but were mainly concentrated over distended cisternae and condensing vacuoles located on the exit side of the stacks. At this time the RER was noticeably less labeled, and labeled granules were very few in number. Thus the concentrative function that the Golgi complex plays in the packaging of secretory product had become evident.

By 36 min chase (Fig. 9) the concentrated secretory material associated with cisternae and condensing vacuoles on the Golgi exit face was heavily labeled. Multiple concentrative sites were evident in single acinar cells. The RER had few residual grains and secretory granules were still devoid of label.

After 56 min and especially after 86 min (Fig.

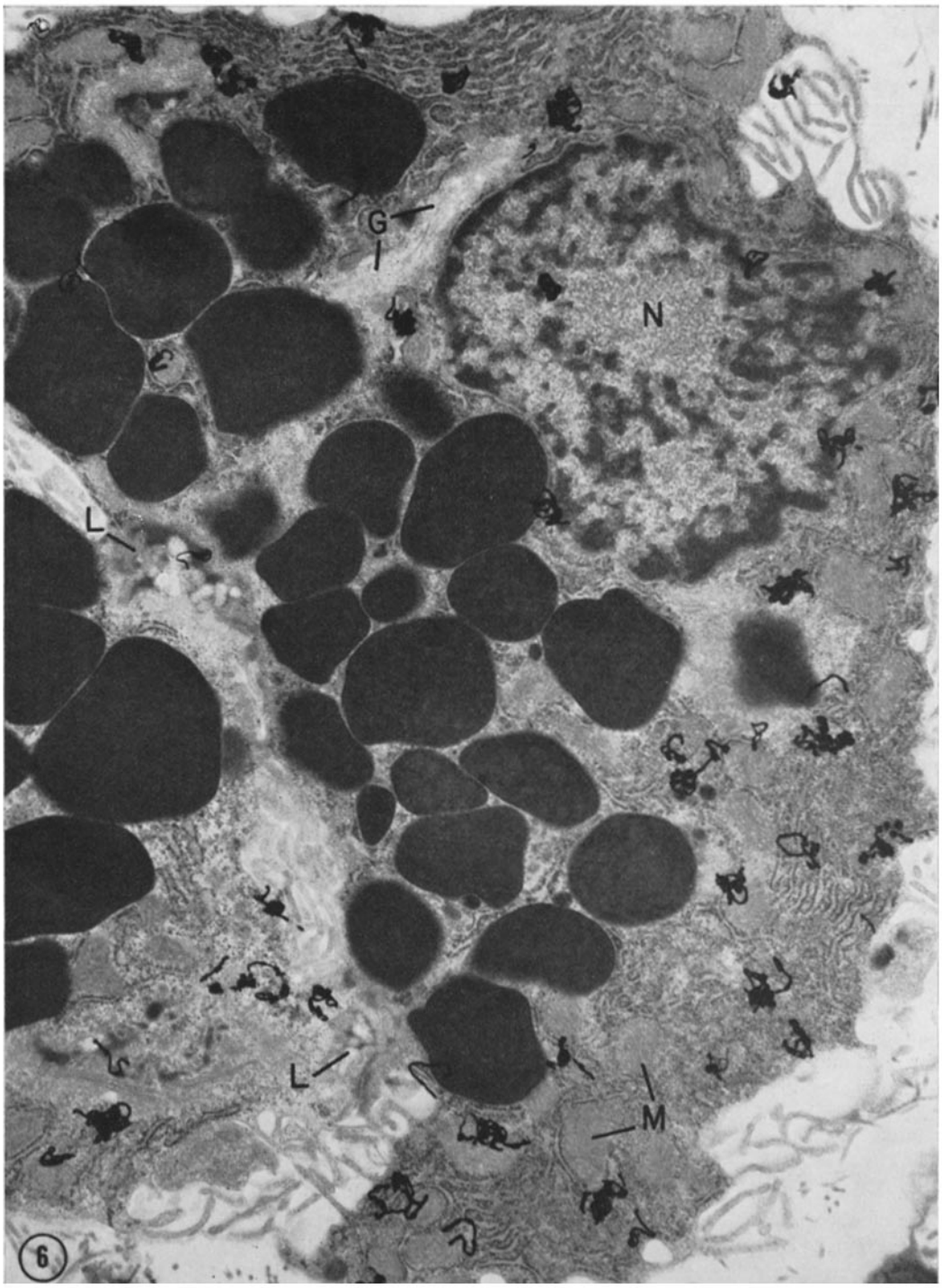

FIGURE 6 Radioautograph of an acinar cell after 1 min chase incubation after a 4 min pulse with leucine-^{3}H. The radioautographic grains are located almost exclusively over the RER. Note the two profiles of acinar lumina (*L*) associated with this cell. The nucleus (*N*), RER cisternae and particularly the intercellular spaces show the effect of water removal by the hypertonic 10% formaldehyde fixation. Mitochondrion (*M*); Golgi complex (*G*). × 20,000.

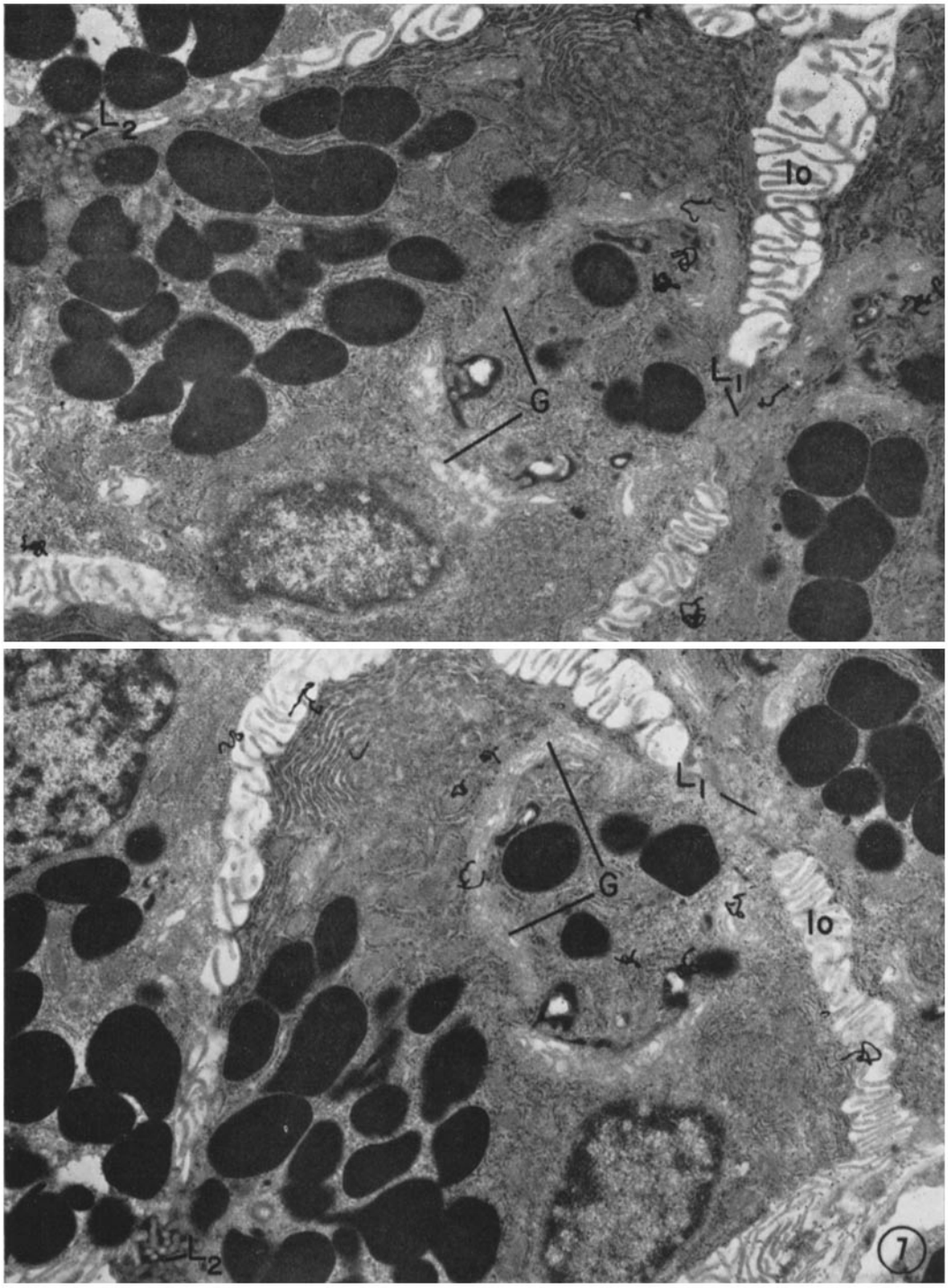

FIGURE 7 Radioautograph of two nearly successive sections of the same cells after 11 min chase incubation. Note that the long stacks of Golgi cisternal elements (*G*) are labeled and that labeling patterns are different in the two sections. The extensive Golgi complex seen in the two sections is probably associated with the acinar lumen L_1. Its position and orientation relative to the main mass of secretion granules of the cell appear to be the reverse of those typically observed in the guinea pig pancreas. The main mass of granules is polarized toward the acinar lumen L_2. It may extend over the Golgi complex in a different plane and/or may be associated with another Golgi complex located at a different level within the cell. Lateral outfoldings (*lo*). × 12,000.

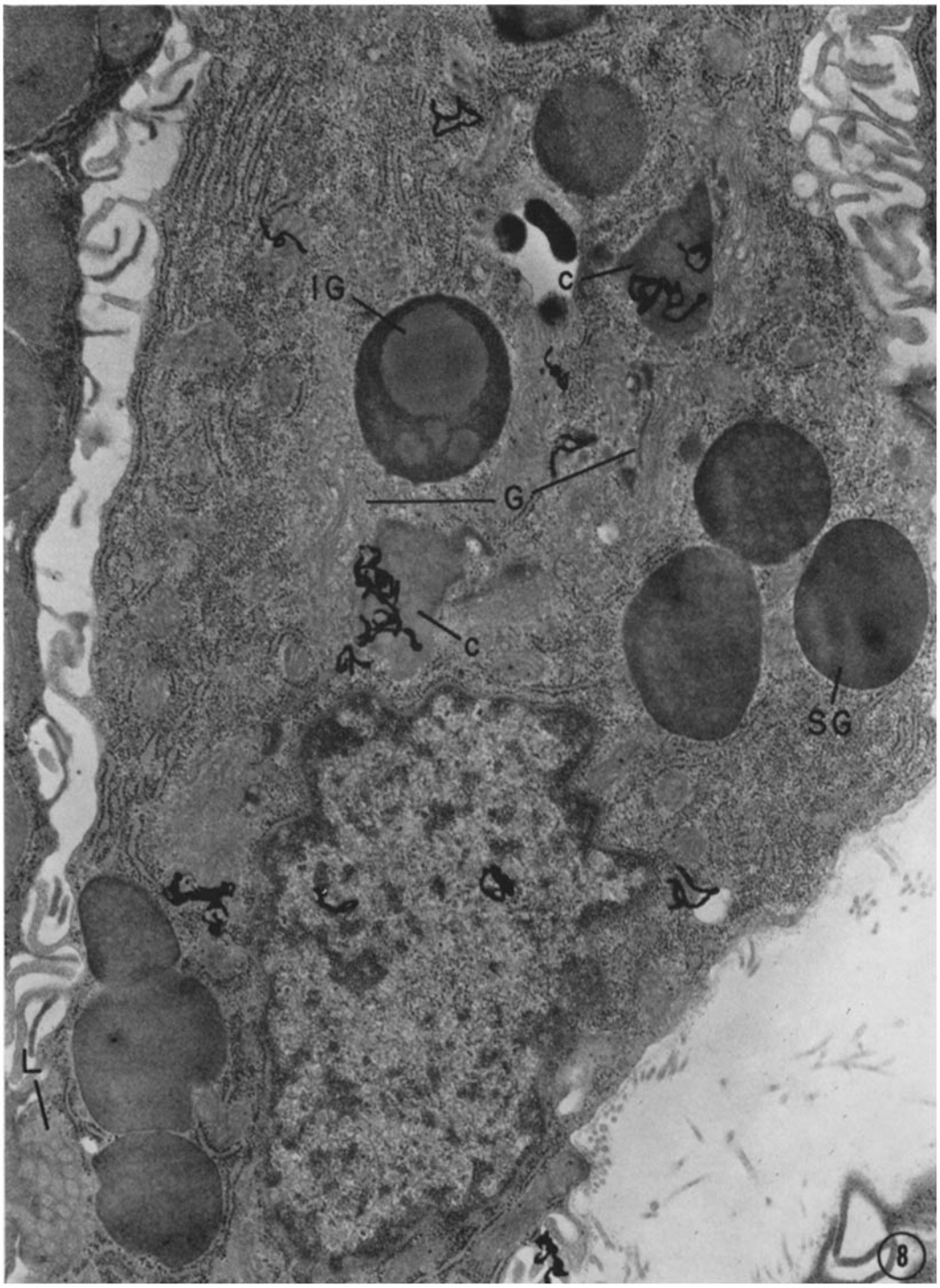

FIGURE 8 Radioautograph of a parotid acinar cell after 26 min incubation in chase medium. The concentrative function of the Golgi complex has become evident since numerous radioautographic grains are seen over condensing vacuoles (*c*). The label has migrated in large part from the RER, but secretory granules (*SG*) are still unlabeled. Golgi cisternae (*G*); immature granules (*IG*); acinar lumen (*L*). × 20,000.

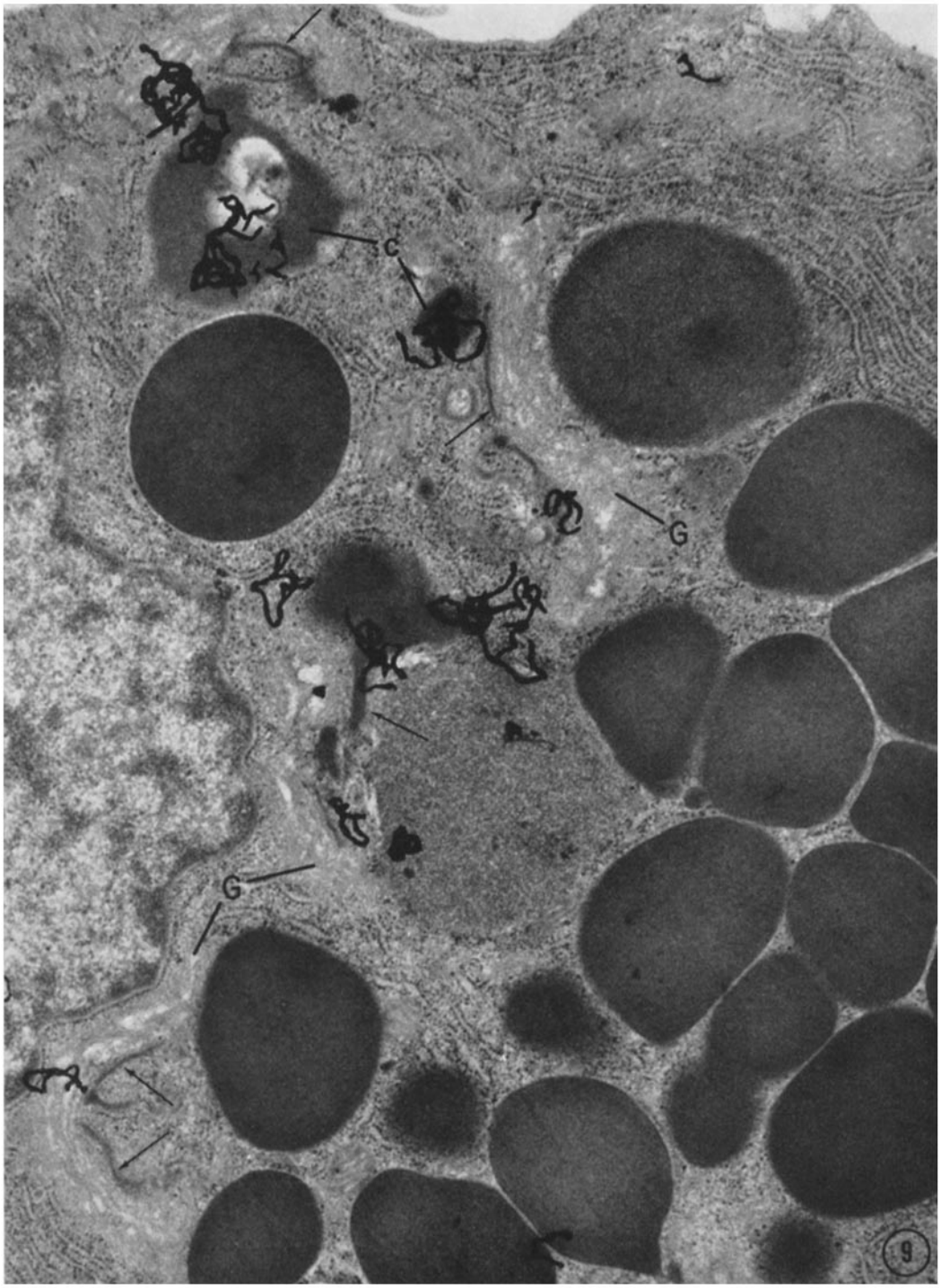

FIGURE 9. Radioautograph of a portion of an acinar cell 36 min postpulse. Multiple concentrative sites on the exit side of the Golgi complex are indicated by the presence of cisternae and condensing vacuoles containing content of high density (arrows). The label marks these condensing vacuoles (*c*) and exit sides of the stacks. Label remaining over the RER is minimal. Golgi cisternae (*G*). × 31,000.

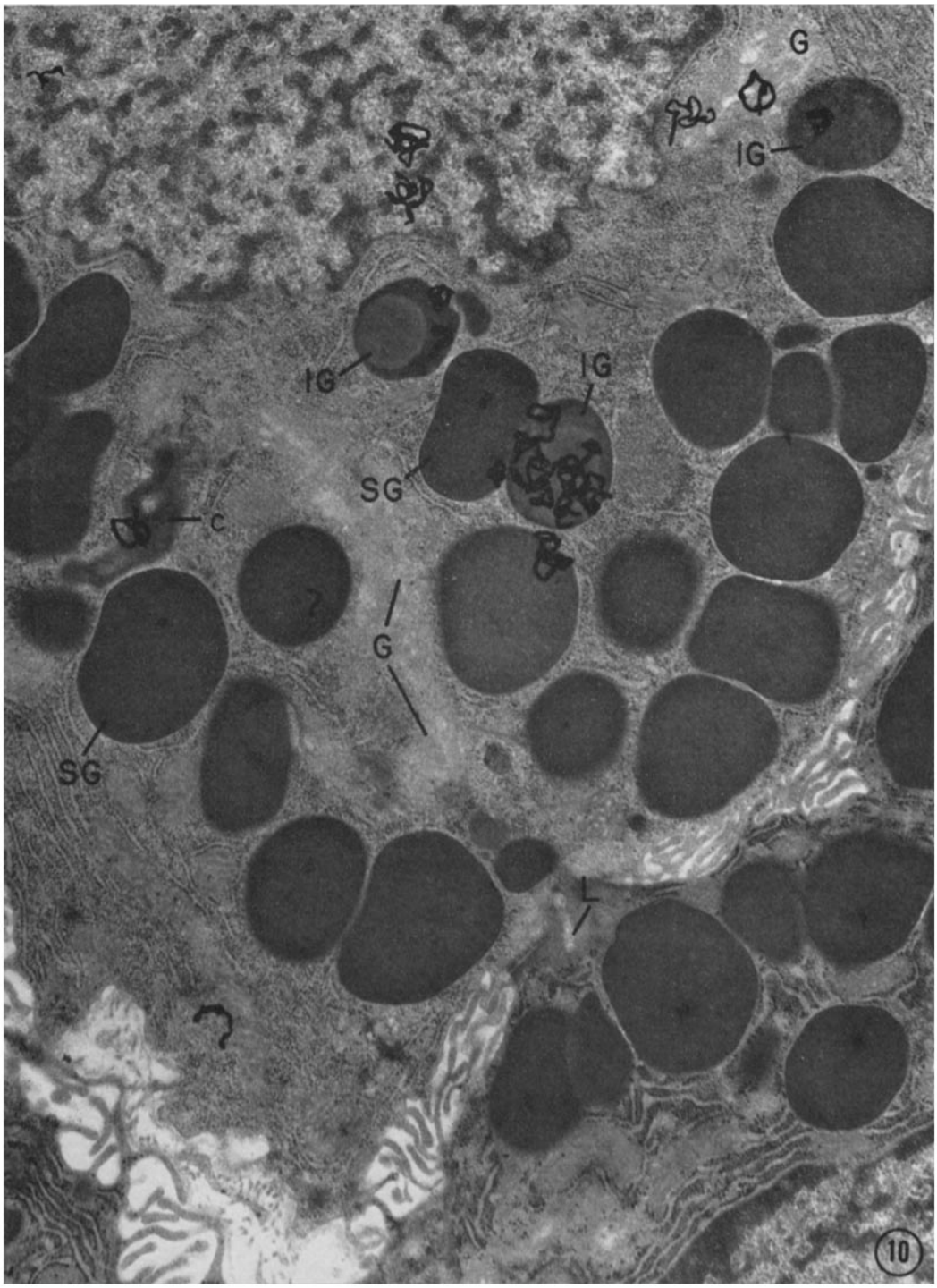

FIGURE 10 Radioautograph of part of an acinar cell after 86 min chase incubation. Immature granules (*IG*) recognizable by their heterogeneously packed content are highly labeled while the Golgi complex (cisternae [*G*] and condensing vacuoles [*c*]) is partially cleared of labeled proteins. Mature secretory granules (*SG*) remain unlabeled. Lumen (*L*). × 17,000.

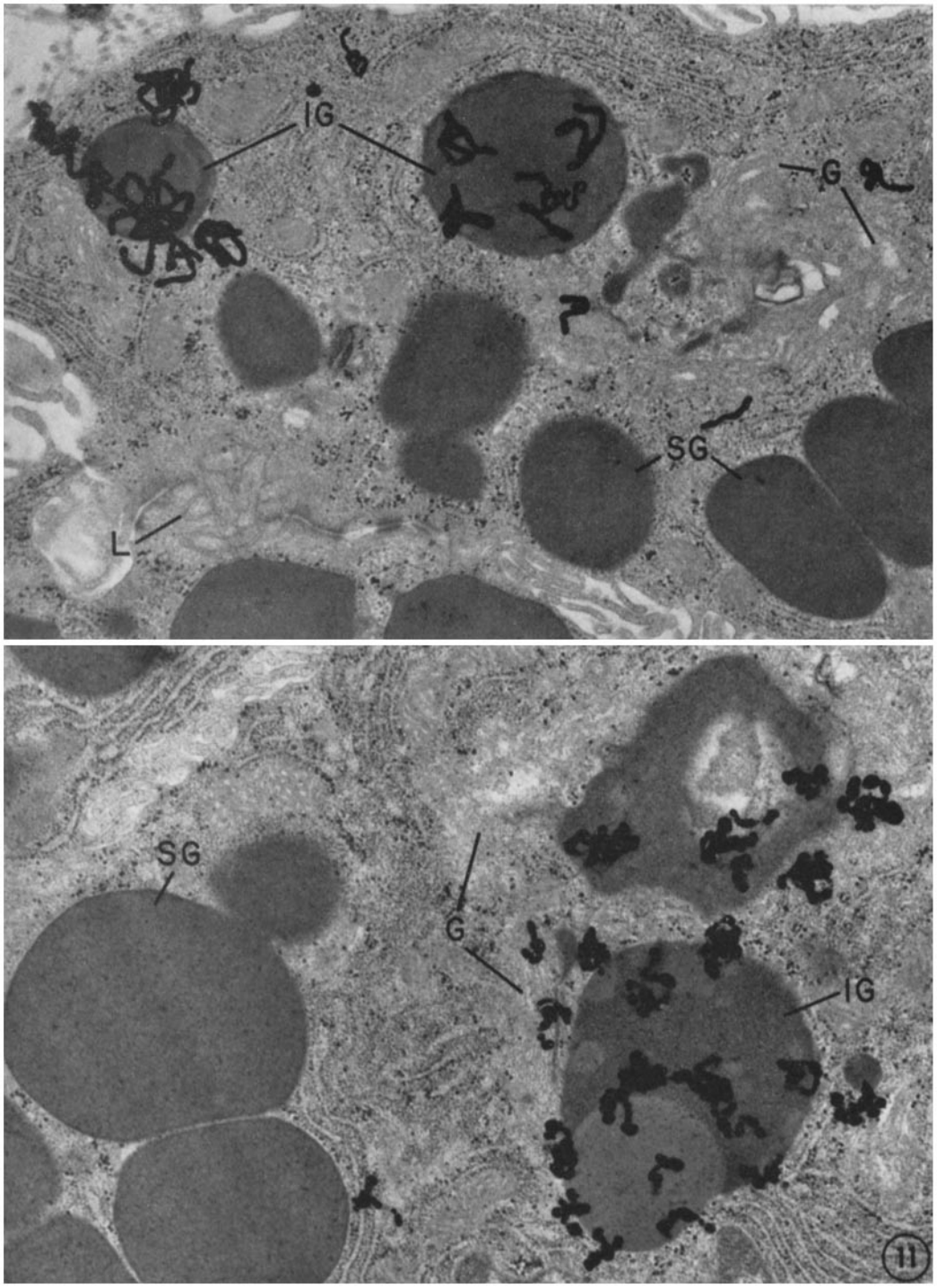

FIGURE 11 Two radioautographs of portions of acinar cells 116 min postpulse. They demonstrate the retardation of intracellular transport of secretory proteins in the rabbit parotid relative to the guinea pig pancreas. Mature secretion granules (*SG*), highly labeled at this time in pancreatic exocrine cells, still are devoid of label, while immature granules (*IG*) are marked by highly concentrated radioautographic grains. Golgi cisternae (*G*); lumen (*L*). Both figures: × 20,000.

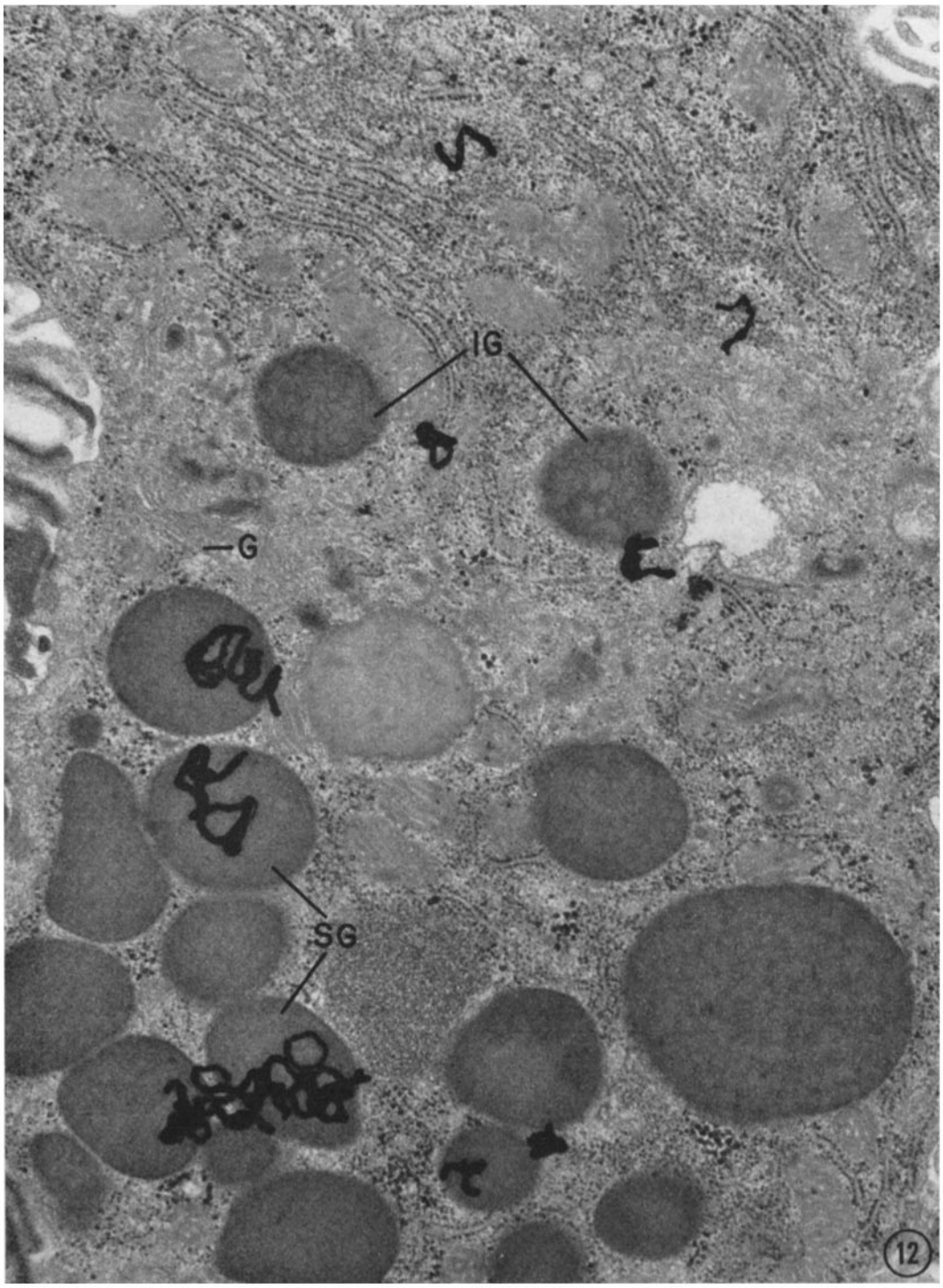

FIGURE 12 Radioautograph of part of a parotid acinar cell chase-incubated for 176 min. Radioautographic grains are concentrated over secretory granules (*SG*) that have attained homogeneous packing of their content, have joined the mass of storage granules of the cell, and hence are considered mature secretion granules. The immature granules (*IG*) are no longer highly labeled, indicating that the crest of the wave of incorporated label has passed this stage of intracellular transport. Golgi cisternae (*G*). × 25,000.

10) and 116 min (Fig. 11) chase, the label was concentrated over granules which: (*a*) were close to, but not directly associated with, the Golgi region, (*b*) had not yet joined the cells' granule storage population, and (*c*) possessed an obvious substructure, possibly reflecting uneven concentration of secretory product. On the basis of these three criteria and especially of the time of their labeling, we consider that these structures are immature secretory granules. After 116 min chase some label still trailed over the Golgi complex, but silver grains were not yet associated in significant numbers with mature, homogeneously dense granules.

After 176 min (Fig. 12) and later, the label was found over granules which had attained homogeneous density and had become part of the cell's accumulated granule population, but most of the labeled granules were still basally located (removed from the cell apex) within this population. Radioautographic grains overlying immature granules markedly decreased from 176 min to 356 min chase.

Extensive concentration of the secretory product in condensing vacuoles and immature and mature granules was indicated by the presence of a large number of radioautographic grains associated with individual structural units.

To quantitate the radioautographic grain distribution over the various subcellular components, grain counts were performed on low magnification electron micrographs (Table III and Fig. 13). The wavelike passage of pulse-labeled secretory protein through intracellular compartments: RER → Golgi → immature granules → mature secretion granules is readily observed. After 1 min chase the bulk of the radioactive label was found in the RER (~78%). At subsequent times during chase incubation there was a progressive decrease of label associated with the RER to a level of about 20% of the total grains. This residual label presumably represents nonexportable protein (34).

With the decrease of label associated with the RER there was a concomitant increase in Golgi-associated label which reached a maximal level (62%) by 36 min chase. At this time labeled secretory protein was maximally concentrated in vacuoles in direct contact with the exit side of the Golgi complex. After prolonged chase very few radioautographic grains remained over the Golgi complex, indicating efficient drainage.

The Golgi-associated condensing vacuoles developed into heavily labeled immature granules that were somewhat removed from the concave face of the Golgi complex. 50% of the grains were localized over such immature granules by 116 min chase incubation. Granule maturation and migration into the accumulated granule population proceeded for the duration of the chase

TABLE III

Distribution of Radioautographic Grains over Cell Components

% of radioautographic grains* (chase incubation after a 4 min pulse)

	1 min	6 min	11 min	16 min	26 min	36 min	56 min	86 min	116 min	176 min	236 min	356 min
Rough endoplasmic reticulum	77.7	66.7	58.6	49.8	31.8	24.4	19.4	19.2	17.7	22.5	25.7	19.1
Golgi complex												
Periphery including entrance cisternae	6.7	11.8	20.5	24.1	27.4	22.0	16.0	8.3	7.5	5.2	1.3	2.2
Exit cisternae and condensing vacuoles	0.9	3.5	1.3	3.3	22.0	40.3	35.9	19.2	16.1	4.2	2.8	0.9
Immature secretion granules	—	1.4	0.9	1.6	3.5	4.2	18.4	40.4	49.4	16.9	9.3	2.9
Mature secretion granules	6.7	6.1	6.2	7.4	6.8	2.8	4.5	7.1	7.4	35.2	49.5	58.5
Nuclei	3.3	4.9	6.4	7.9	6.4	5.2	3.3	3.9	4.7	10.3	8.3	12.4
Mitochondria	4.6	4.7	6.6	5.9	2.1	1.0	2.4	1.8	—	4.7	2.6	3.6
No. of grains counted	817	491	454	1740	971	1480	749	661	612	213	540	582

Underlined numbers indicate maximum accumulation of grains over the corresponding cell component.
* These data were obtained in two overlapping experiments.

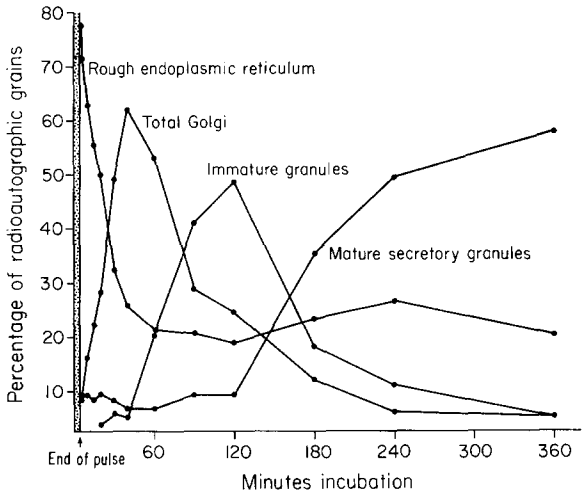

FIGURE 13 Wavelike movement of pulse-labeled secretory protein through intracellular compartments. A plot of the quantitative data of Table III for cellular components involved in transport. Summation of percentages at each time point shows that 75–80% of the incorporated label moves with the wave against the RER background of 20%.

past 116 min. The thoroughness of conversion of immature granules (Table III and Fig. 13) suggested that the intracellular transport system is completely functional throughout the 6 hr chase.

The labeling of nuclei and mitochondria was generally low and variable (nuclei: 3.3–12.4% and mitochondria: <1–6.6%). No significant label was ever seen in acinar lumina, corroborating the observation of extremely few labeled granules at the cell apex.

DISCUSSION

Earlier morphological and biochemical studies of the parotid gland were made on rats (8–13, 15–17, 35–54). We chose rabbits for the following reasons: (*a*) their parotids are compact, well-encapsulated glands, hence they can be removed more easily and cleanly than the diffuse parotids of rats; (*b*) the glands are large enough so that parotid tissue from a single rabbit is sufficient for most biochemical experiments; (*c*) rabbit parotids have a reasonably high content of amylase; and (*d*) there are no previous studies of the parotid in this species.

An adequate in vitro incubation system should be capable of maintaining for several hours the structural integrity of the tissue and its ability to synthesize proteins, and should allow satisfactory control of the exposure of the tissue to chemical substituents. In the system used, we have shown that it is possible to substitute a labeled protein precursor (L-leucine-^{3}H) for its counterpart (L-leucine-^{1}H) for a short, well-defined time (pulse), to dilute out subsequently the unincorporated leucine-^{3}H (chase), and thereby to satisfy the conditions required for a study of the kinetics of intracellular transport of secretory proteins labeled during the pulse. Since tissue from a single rabbit is used for all time points, differences due to individual variations among animals are avoided. To reduce damage to acinar cells we have used dissected lobules instead of tissue slices, and we have substituted a tissue culture medium, i.e. Nutrient Mixture F 12, for the amino acid–supplemented Krebs-Ringer-bicarbonate medium used in references 5 and 6. With these modifications it was possible to extend the chase incubation by 3–4 hr past the duration achieved in our previous experiments on pancreatic slices from the guinea pig (5, 6). In other respects, i.e. initial rate of incorporation of labeled leucine and efficiency of chase, the two systems are comparable.

In interpreting our radioautographic findings we have assumed that labeled amino acids are much more rapidly incorporated into exportable proteins than into nonexportable proteins produced for intracellular use. This assumption is supported by: (*a*) the lobule discharge experiment which demonstrates that at least two-

thirds of the leucine-labeled protein is secretory protein as assayed by export under stimulation, and (*b*) the data in Fig. 13 which show that most of the labeled protein (~75%) moves as a single wave through a series of intracellular compartments against a low radioactive background which primarily marks the basal region of the cell and which is taken to represent, in large part, nonexportable proteins.

Our results show that the transport of secretory proteins in the parotid acinar cell of the rabbit is vectorial and follows the same pathway: RER → Golgi complex → storage granules, as in the pancreatic exocrine cell of the guinea pig. The drainage of the first two compartments is quite efficient, and the rates of outflow from the RER are practically identical in the two cell types: maximal labeling of condensing vacuoles is reached in both cases after 36–37 min chase (compare our Table III with Table II in reference 6). In comparing transport through the Golgi complex, differences in the appearance of this organelle in the two glandular cells must be considered. The general organization is similar but the relative amount of various Golgi elements and their topography is significantly different. In the pancreatic exocrine cell of the guinea pig the peripheral Golgi vesicles (which have been implicated in transport from the transitional elements of the RER to condensing vacuoles [6]) are numerous, while the stacks of Golgi cisternae are narrow and separated from one another by relatively large intervals through which the small vesicles could reach the condensing vacuoles; the latter are usually centrally located in the complex. In the parotid acinar cell of the rabbit there are relatively few vesicles at the periphery of the complex, and the unusually broad cisternal stacks appear to be separated from one another by few corridors of potential access to the condensing vacuoles. These features suggest a possible involvement of the stacked cisternae in the transport of parotid secretory products, and the suggestion is further strengthened by the following observations:

(*a*) There is morphological evidence that secretory products are concentrated in the stacked cisternae of the Golgi complex in many glandular cells (23, 30, 31, 55–59).

(*b*) In the rat parotid, the cytochemical observations of Herzog and Miller (13) suggest the existence of an increasing entry-exit concentration gradient for peroxidase in the cisternae of the Golgi stacks. Peroxidase is one of the enzymes secreted by the rat parotid.

(*c*) Continuous secretagogue stimulation of guinea pig pancreatic slices leads to a structural and functional reorganization of the Golgi complex of the exocrine cells. The number of peripheral vesicles decreases, stacks of Golgi cisternae are considerably enlarged, typical condensing vacuoles practically disappear, and radioautographic evidence indicates that concentration of secretory product occurs in the distal cisternae (and associated vacuoles) of the Golgi stacks (18).

(*d*) In the acinar cells of the parotid occasional connections (Fig. 2) are found between adjacent cisternae within the stacks. Similar connections have already been noted in other cell types (60).

Our results indicate that during the transport of secretory proteins the label appears at the periphery of the Golgi complex over vesicles as well as over stacked cisternae, but the radioautographic resolution attained is not sufficient to establish that transport is indeed routed through the Golgi cisternae and to define a concentration gradient within the Golgi stacks.

On the basis of our kinetic findings we can recognize an entrance side and an exit side for the Golgi complex, even if we cannot yet resolve the actual sites of entry. For this reason we have used these expressions throughout the text instead of convex *versus* concave face and proximal *versus* distal face which are frequently in contradiction with local morphology and topography. We prefer this terminology to immature *versus* mature face since, in our case, we do not have evidence concerning the maturation processes of the Golgi membranes themselves.

Past the condensing vacuole stage, intracellular transport in the acinar cell of the rabbit parotid slows considerably relative to its pancreatic counterpart, and an additional step becomes evident in the maturation process of the condensing vacuoles. The step is represented by immature secretory granules removed from the exit side of the cisternal stacks but still located in the vicinity of the Golgi complex. Immature granules possess morphologically distinguishable, heterogeneously packed secretory product and show high density of radioautographic label by 86 and 116 min chase. Since in the acinar cells of the rabbit parotid, immature secretory granules are of comparable or larger size than mature

secretory granules, and since Golgi peripheral vesicles are small and few in number, there is no morphological evidence in this species for the intracellular existence of the small-sized, slowly sedimentable (4000 *g* and 15,000 *g*) intermediate structures postulated in the development of the secretory granules in the parotid of the rat (12).

Labeled, homogeneously packed mature secretory granules (accounting for 35% of the radioautographic grains) begin to appear in parotid acinar cells by 176 min chase, whereas pancreatic zymogen granules are already labeled to a comparable extent (accounting for 33% of the radioautographic grains) by only 57 min chase (see Table II in reference 6). Thus maturation of secretory granules is a prolonged process in the parotid. Furthermore, whereas labeled pancreatic zymogen granules readily become evenly distributed throughout each cell's granule population (Fig. 13 in reference 6), the labeled parotid mature secretory granules fail to become randomized in each cell's granule accumulation, even after postpulse incubation for 356 min. Generally the labeled granules remain proximally located in the apical accumulation often adjacent to other labeled granules as if tight packing restricts granule movement relative to one another. Very rarely are labeled granules seen at cellular apices, and no significant label appears in the parotid acinar lumina even by 356 min chase in contrast to the pancreatic counterparts which are significantly labeled by 116 min chase.

Thus the parotid acinar cell of the rabbit synthesizes, transports, and stores secretory proteins in the same way as the pancreatic exocrine cell of the guinea pig. The pathway followed in transport is identical, although temporally expanded during granule maturation. Parotid acinar cells maintain a much larger stored granule population than do pancreatic exocrine cells in animals fed *ad libitum*, and the granule turnover time (synthesis to release) is probably greatly prolonged in this gland since release appears not to be a random process. It should be pointed out, however, that the kinetics of release and possibly storage might be regulated in vivo by changes in environmental factors (nerve stimulation, masticatory movements [52]) which do not operate in vitro.

The kinetics of intracellular transport in the rabbit parotid established in this study can be used as a guide for future cell fractionation studies.

We wish to thank Mrs. Louise E. Castle for her excellent assistance during surgical removal of parotid glands and in the preparation of this manuscript.

This investigation was supported in part by Public Health Service Research Grant AM-10928 from the National Institute of Arthritis and Metabolic Diseases.

Received for publication 13 October 1971, and in revised form 17 December 1971.

REFERENCES

1. WARSHAWSKY, H., C. P. LEBLOND, and B. J. DROZ. 1963. *J. Cell Biol.* **16**:1.
2. VAN HEYNINGEN, H. E. 1964. *Anat. Rec.* **148**:485.
3. PALADE, G. E., P. SIEKEVITZ, and L. G. CARO. 1962. *In* Ciba Foundation Symposium on the Exocrine Pancreas. A. V. S. de Reuck and M. P. Cameron, editors. J. and A. Churchill Ltd., London. 23.
4. CARO, L. G., and G. E. PALADE. 1964. *J. Cell Biol.* **20**:473.
5. JAMIESON, J. D., and G. E. PALADE. 1967. *J. Cell Biol.* **34**:577.
6. JAMIESON, J. D., and G. E. PALADE. 1967. *J. Cell Biol.* **34**:597.
7. MELDOLESI, J., J. D. JAMIESON, and G. E. PALADE. 1971. *J. Cell Biol.* **49**:130.
8. PARKS, H. F. 1961. *Amer. J. Anat.* **108**:303.
9. PARKS, H. F. 1962. *J. Ultrastruct. Res.* **6**:449.
10. AMSTERDAM, A., I. OHAD, and M. SCHRAMM. 1969. *J. Cell Biol.* **41**:753.
11. BDOLAH, A., R. BEN-ZVI, and M. SCHRAMM. 1969. *Arch. Biochem. Biophys.* **104**:58.
12. SCHRAMM, M., and A. BDOLAH. 1964. *Arch. Biochem. Biophys.* **104**:67.
13. HERZOG, V., and F. MILLER. 1970. *Z. Zellforsch. Mikrosk. Anat.* **107**:403.
14. HAM, R. G. 1965. *Proc. Nat. Acad. Sci. U. S. A.* **53**:288.
15. SIMSON, J. V. 1969. *Z. Zellforsch. Mikrosk. Anat.* **101**:175.
16. BARKA, T. 1971. *Exp. Cell Res.* **64**:371.
17. BYRT, P. 1966. *Nature (London).* **212**:1212.
18. JAMIESON, J. D., and G. E. PALADE. 1971. *J. Cell Biol.* **50**:135.
19. GRAHAM, R. C., and M. J. KARNOVSKY. 1966. *J. Histochem. Cytochem.* **14**:291.
20. LUFT, J. H. 1961. *J. Biophys. Biochem. Cytol.* **9**:409.
21. RICHARDSON, K. C., J. JARETT, and E. H. FINKE. 1960. *Stain Technol.* **35**:313.
22. VENABLE, J. H., and R. COGGESHALL. 1965. *J. Cell Biol.* **25**:407.

23. WUHR, P., A. HERSCOVICS, and C. P. LEBLOND. 1969. *J. Cell Biol.* **43**:289.
24. ASHLEY, C. A., and T. PETERS. 1969. *J. Cell Biol.* **43**:237.
25. CARO, L. G., and R. P. VAN TUBERGEN. 1962. *J. Cell Biol.* **15**:173.
26. BRAY, G. A. 1960. *Anal. Biochem.* **1**:279.
27. BERNFELD, P. 1955. *In* Methods in Enzymology. S. P. Colowick and N. O. Kaplan, editors. Academic Press Inc., New York. **1**:149.
28. LOWRY, O. H., O. J. ROSEBROUGH, A. L. FARR, and R. J. RANDALL. 1951. *J. Biol. Chem.* **193**:265.
29. BURTON, K. 1956. *Biochem. J.* **62**:315.
30. NEUTRA, M., and C. P. LEBLOND. 1966. *J. Cell Biol.* **30**:119.
31. NEUTRA, M., and C. P. LEBLOND. 1966. *J. Cell Biol.* **30**:137.
32. ZIMMERMAN, K. W. 1927. *In* Handbuch der Mikroskopischen Anatomie des Menschen. W. Möllendorff, editor. Springer-Verlag KG., Berlin. **5**(1):139.
33. JAMIESON, J. D., and G. E. PALADE. 1968. *J. Cell Biol.* **39**:580.
34. SIEKEVITZ, P., and G. E. PALADE. 1960. *J. Biophys. Biochem. Cytol.* **7**:619.
35. SCHRAMM, M., and D. DANON. 1961. *Biochim. Biophys. Acta.* **50**:102.
36. HAND, A. 1971. *Amer. J. Anat.* **130**:141.
37. HAND, A. 1970. *J. Cell Biol.* **47**:540.
38. BABAD, H., R. BEN-ZVI, A. BDOLAH, and M. SCHRAMM. 1967. *Eur. J. Biochem.* **1**:96.
39. BATZRI, S., A. AMSTERDAM, Z. SELINGER, I. OHAD, and M. SCHRAMM. 1971. *Proc. Nat. Acad. Sci. U. S. A.* **68**:121.
40. SCHRAMM, M., B. EISENKRAFT, and E. BARKAI. 1967. *Biochim. Biophys. Acta.* **135**:44.
41. BDOLAH, A., and M. SCHRAMM. 1965. *Biochem. Biophys. Res. Commun.* **18**:452.
42. SCHRAMM, M., R. BEN-ZVI, and A. BDOLAH. 1965. *Biochem. Biophys. Res. Commun.* **18**:446.
43. SCHRAMM, M. 1968. *Biochim. Biophys. Acta.* **165**:546.
44. SCHRAMM, M., and E. NAIM. 1970. *J. Biol. Chem.* **245**:3225.
45. SELINGER, Z., and E. NAIM. 1970. *Biochim. Biophys. Acta.* **203**:335.
46. SELINGER, Z., E. NAIM, and M. LASSER. 1970. *Biochim. Biophys. Acta.* **203**:326.
47. FEINSTEIN, H., and M. SCHRAMM. 1970. *Eur. J. Biochem.* **13**:158.
48. AMSTERDAM, A., M. SCHRAMM, I. OHAD, Y. SOLOMON, and Z. SELINGER. 1971. *J. Cell Biol.* **50**:187.
49. WALLACH, D., and M. SCHRAMM. 1971. *Eur. J. Biochem.* **21**:433.
50. BARKA, T. 1970. *Exp. Cell Res.* **61**:290.
51. ROBINOVITCH, M. R., L. M. SREEBNY, and E. A. SMUCKLER. 1968. *J. Biol. Chem.* **243**:3441.
52. SREEBNY, L. M., D. A. JOHNSON, and M. R. ROBINOVITCH. 1971. *J. Biol. Chem.* **246**:3879.
53. GRAND, R. J., and P. R. GROSS. 1969. *J. Biol. Chem.* **244**:5608.
54. GRAND, R. J., and P. R. GROSS. 1970. *Proc. Nat. Acad. Sci. U. S. A.* **65**:1081.
55. ESSNER, E. 1971. *J. Histochem. Cytochem.* **19**:216.
56. BAINTON, D. F., and M. G. FARQUHAR. 1966. *J. Cell Biol.* **28**:277.
57. BAINTON, D. F., and M. G. FARQUHAR. 1968. *J. Cell Biol.* **39**:299.
58. BAINTON, D. F., and M. G. FARQUHAR. 1970. *J. Cell Biol.* **45**:54.
59. FARQUHAR, M. G. 1971. *In* Subcellular Organization and Function in Endocrine Tissue. H. Heller and K. Lederis, editors. Cambridge University Press, London. 79.
60. PALAY, S. L., and G. E. PALADE. 1955. *J. Biophys. Biochem. Cytol.* **1**:69.